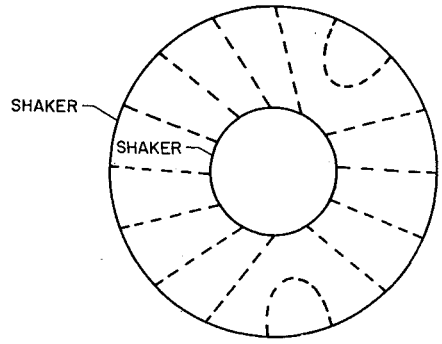

Fig. 2 Sketch of typical nodal pattern for free-free frustums as viewed along the longitudinal axis.

Thus far, no adequate analysis for prediction of the natural frequencies of frustums of the type under investigation with free-free boundary conditions is known to the authors. An analysis[4] has been developed, however, which predicts a difference in the number of circumferential waves for radially stiffened frustums fixed (imbedded) at the major diameter.

References 2 and 3 develop frequency equations for fixed-free frustums. Two frequency equations are derived, one for inextensional (i.e., bending or flexure) and another for extensional or membrane vibrations. Shell displacements are assumed for each case and substituted into the potential and kinetic energy expressions that are then set equal. The extensional analysis results in a rather complicated matrix that can be solved for the dimensionless frequency parameter Δ_e, which is related to the extensional frequencies as follows:

$$\Delta_e = (1 - \nu^2)\rho\lambda^2 l^2(2\pi f_e)^2/E \tag{1}$$

Inextensional frequencies were calculated from the equation

$$f_i = \frac{hn(n^2 - 1)}{4\pi r_0^2 \cos\alpha}\left[\frac{E}{3\rho(1 - \nu^2)}\right]^{1/2}\left(\frac{N}{D}\right)^{1/2} \tag{2}$$

where N and D are dimensionless geometric parameters.[2, 3] The frequency parameter Δ_i is then obtained by replacing f_e in Eq. (1) with f_i obtained from Eq. (2).

The theoretical frequency parameter was then formed from the relation

$$(\Delta)^{1/2} = (\Delta_i + \Delta_e)^{1/2} \tag{3}$$

A comparison of the experimental and theoretical value of the frequency parameter for the fixed-free frustums is shown in Fig. 3.

IV. Concluding Remarks

Results of Rayleigh-type vibration analyses[2, 3] have shown good agreement with experimental results for conical frustum shells with fixed-free ends. No adequate theory is known to the authors for predicting the mode shapes and natural frequencies of free-free frustums. An essential ingredient of desired analysis is its generality to take into account the difference in the number of circumferential waves found at the major and minor diameters of the shell. In addition, a need for better analytical procedures exists for the determination of the dynamic behavior of various cylinder-cone combinations subjected to vibratory loads under all boundary conditions.

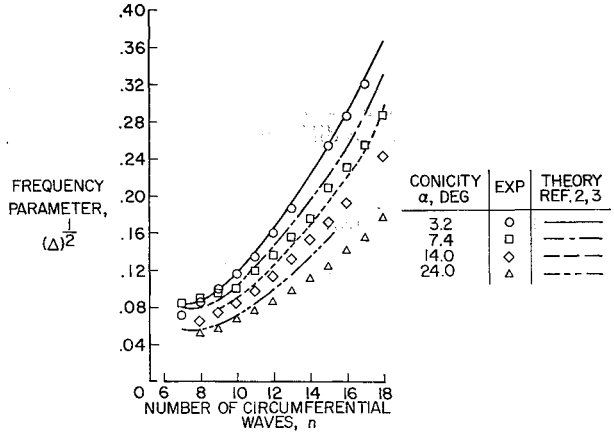

Fig. 3 Experimental and theoretical frequency characteristics of conical frustum shells with fixed-free end conditions, $m = 1$.

References

[1] Gros, C. G. and Forsberg, K., "Vibrations of thin shells: A partially annotated bibliography," Lockheed Special Bibliography SB-63-43 (April 1963).

[2] Platus, D. H., "Study on bell-mode vibrations of conical nozzles, first quarterly progress report," Aerojet-General Rept. 0660-1, 3-14 (August 1962).

[3] Platus, D. H., "Study on bell-mode vibrations of conical nozzles, second quarterly progress report," Aerojet-General Rept. 0660-01-2, 3-22 (November 1962).

[4] McGrattan, R. J. and North, E. L., "Shell mode coupling," General Dynamics, Electric Boat Rept. U411-63-005 (March 1963).

Use of Stress Relaxation Tests to Characterize Time Dependencies of a Composite Solid Propellant

JOSEPH H. STOKER*
Thiokol Chemical Corporation, Brigham City, Utah

Introduction

TO define or characterize the behavioral characteristics of a viscoelastic material accurately, its responses to an applied load must be determined as a function of strain rate, time, and temperature. These characteristics may be determined by means of a stress relaxation test. This test requires an instantaneous specimen extension and the measurement of the diminishing force required to maintain the elongation constant over an extended time period.

Experimental Procedure

The samples used in the stress relaxation determinations were cast cylindrical specimens, designed for a constant gage length, with a 0.5-in. diam in the necked-down region.[1] The total specimen length was 3.25 in., with a necked-down length of 1.8 in. Aluminum end tabs were bonded to the specimen with Shell 911-S adhesive. The specimens were attached to the statically mounted load cell and the upper, or movable jaw.

Extremely rapid specimen extension was achieved by actuating a gas-operated piston by nitrogen pressure. Both sides of the piston were pressurized. The pressure above the piston was then released rapidly by the actuation of a solenoid valve. The movement of the upper jaw of the apparatus was prevented until the pressure differential was sufficient to break a shear pin and extend the specimen in tension at a rate of 10,500 in./min.

A positive locking cone was machined in the upper plate, with a matching cone on the upper jaw to maintain the required specimen alignment during elongation and to prevent bouncing of the jaw at the end of the stroke. This cone also creates an air cushion that acts as a retarding force at the end of the stroke.

Presented as Preprint 64-131 at the AIAA Solid Propellant Rocket Conference, Palo Alto, Calif., January 29–31, 1964; revision received July 20, 1964.

* Senior Engineer, Development Laboratory, Wasatch Division.

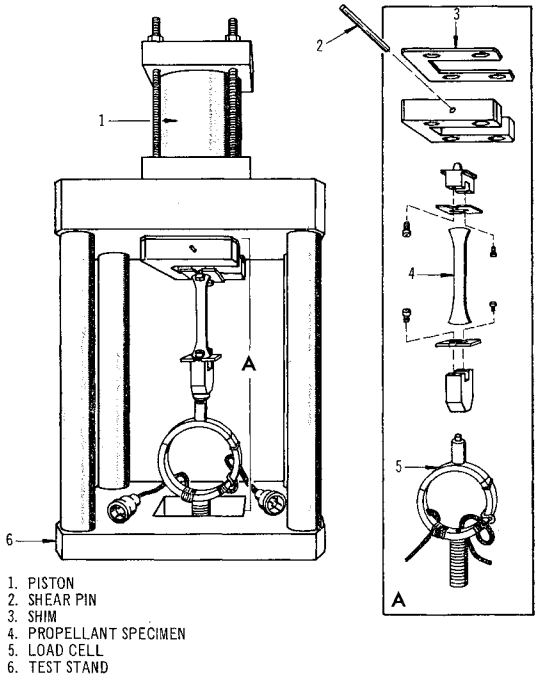

Fig. 1 Stress relaxation test fixture.

Relaxation data were recorded with a dual-beam oscilloscope and a strip chart recorder. The electrical signals were generated by a semiconductor load ring. The elongation was preset by the use of shims (Fig. 1).

Discussion

Experimental data were obtained from tests performed on a composite solid propellant at three temperatures and three moduli. The Joint Army-Navy Air Force (JANAF) moduli of these propellants were 328, 595, and 966 psi. These propellants were tested at 50°, 80°, and 135°F. The experimental results from these tests are shown in Figs. 2–4. The effects of temperature and modulus variation may be seen by examining these figures.

A digital computer program was used to smooth and average the raw stress relaxation data. A logarithmic transformation was accomplished, and the least-squares polynominal fit was taken. An accurate representation of the stress relaxation function was determined to be

$$y = e \exp[A_0 + A_1(\ln t_1) + A_2(\ln t_2)^2 + \ldots A_7(\ln t_7)^7] \quad (1)$$

The best model representation of the composite propellant investigated was a 17-element Wiechert or generalized Maxwell model. The relaxation function $\psi(t)$ for this model may be used according to the method of Gross[2] or Francis and Cantey[3] to perform a viscoelastic transformation and thereby

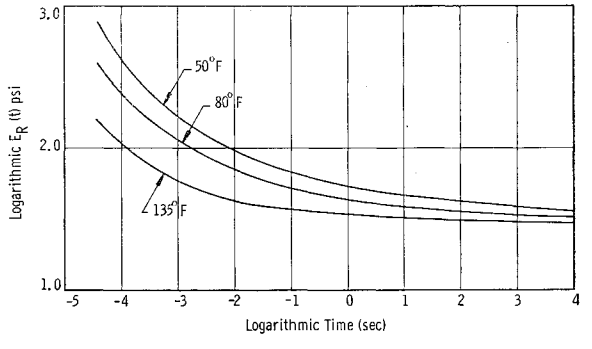

Fig. 2 Logarithmic stress relaxation modulus vs logarithmic times for a typical composite solid propellant (JANAF modulus, 328 psi).

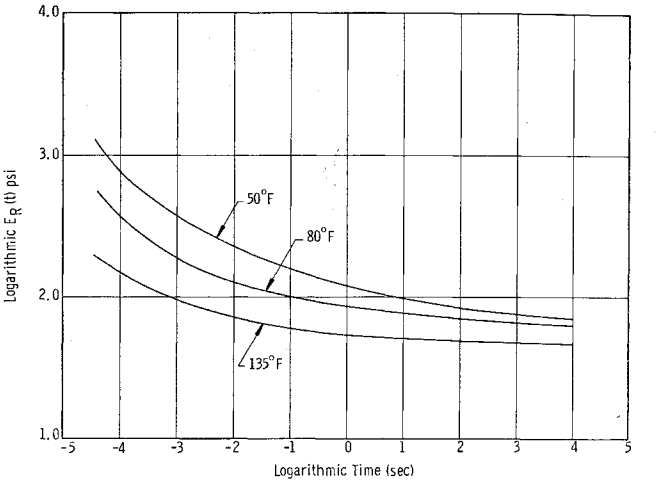

Fig. 3 Logarithmic stress relaxation modulus vs logarithmic times for a typical composite solid propellant (JANAF modulus, 595 psi).

determine the dynamic shear modulus of the material by the relationships of

$$E' = \omega^2 \Sigma \frac{k_i}{(1/\tau_i^2) + \omega^2}$$

$$E'' = \omega \Sigma \frac{k_i}{\tau_i[(1/\tau_i^2) + \omega^2]} \quad (2)$$

where ω is the angular velocity.

Using these equations and the element constants obtained from the experimental stress relaxation determinations, the stress relaxation function was converted to the dynamic shear modulus covering a frequency range of 0.01 to 700 cps. These converted values are shown in Fig. 5, with experimentally derived values for comparative purposes.

Conclusions

To obtain a good viscoelastic transformation from the stress relaxation data to the dynamic shear modulus, the early part of the stress relaxation function had to be measured very accurately. When the specimen deformation was completed in 0.0004 sec, and a decade of time was dropped from the beginning of the stress relaxation function described experimentally, large variations occurred in the calculated values of the dynamic shear modulus. The necessity for a load appli-

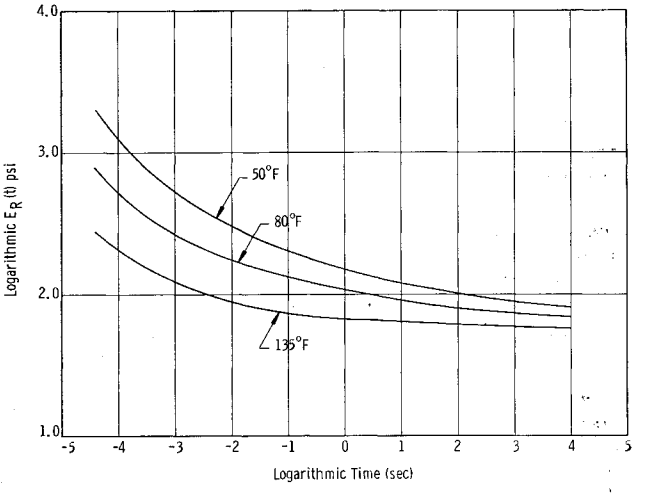

Fig. 4 Logarithmic stress relaxation modulus vs logarithmic times for a typical composite solid propellant (JANAF modulus, 966 psi).

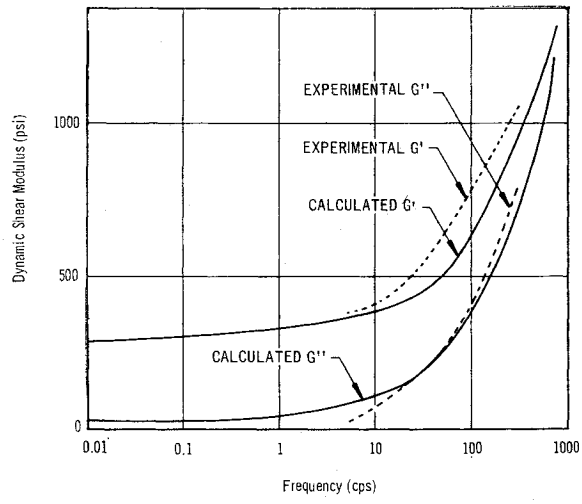

Fig. 5 Dynamic shear modulus vs frequency real (G') and imaginary (G'') parts.

cation within 0.001 sec for accurate viscoelastic transformations was indicated.

During this investigation, the stress relation functions were evaluated. The results of these determinations were used satisfactorily to describe the time dependency of the propellant. This enabled an accurate prediction of the dynamic shear modulus to be made, as is evidenced by the comparison of the calculated and the experimentally determined values.

References

[1] Saylak, D., "The design, fabrication, and evaluation of an end-bonded cylindrical tensile dumbbell for tensile testing composite rocket propellants," Chemical Propulsion Information Agency Bulletin of the 1st Meeting for the Working Group on Mechanical Behavior, p. 54 (December 1962); confidential.

[2] Gross, B., *Mathematical Structure of the Theories of Viscoelasticity* (Publications of the National Institute of Technology, Brazil, 1953), Chap. 3.

[3] Francis, E. C. and Cantey, D., "Solid propellant structural integrity investigation," Lockheed Propulsion Co. TR RTD-TDR-63-1 (May 24, 1963).

A Dynamical Model for Kordylewski Cloud Satellites

FREDERICK V. POHLE*
Adelphi University, Garden City, N. Y.

THE existence of additional natural satellites near the earth has been the object of observational searches[1]; no positive results were announced. In the earth-moon system it is known[2] that the Lagrangian equilateral triangular points (L_4, L_5) are stable points and that matter may remain for a long time in the regions close to such points. Thus it is natural to seek the existence of natural satellites in such regions, and a search was undertaken by K. Kordylewski of the Cracow Observatory in Poland a number of years ago. Success was announced[3–6] with the statement that a pair of thin cloud-like satellites was observed near each stable L point The observational difficulties are extremely great since the clouds are observable on only three nights a month for about two hours between December and April.[7] Although a search has been underway to detect meteoroids within the clouds, none as bright as the twelfth-magnitude has been detected up to the present time.

The existence of dust in the earth-moon space is well known,[8–10] and the object of the present note is to suggest a possible dynamical model[11] to explain the accumulation in the form of clouds observed by Kordylewski. A different explanation has been advanced[12] based on the motion of particles near the stable L points in the form of periodic orbits.

The present model assumes the existence of a small nucleus at the stable L point and the existence of dust moving in the region, near the L point. Since matter can accumulate near the L point, it is at least possible that a small mass, once captured, would remain near the stable point for an indefinite time. This is clearly an assumption at the present time, since the observations have not given positive evidence of the existence of a nucleus. The location of the L point in the earth-moon system is of course determined by the dimensions of that system. Nevertheless, the sphere of influence of the moon is too small for the moon to have an appreciable influence on dust particles near such an L point and, for purposes of a simplified presentation, the effect of the moon will be ignored; a more accurate analysis leads to the same conclusions. The analysis is similar in some respects to the explanation of the gegenschein[13] at the unstable L points (L_1, L_2, L_3).

It will be assumed that the nucleus, as well as the cloud near it, moves in a circular orbit about the earth at a distance equal to that of the lunar distance a in Fig. 1. The small mass is $m(x, y)$ and the plane of the orbit is the (x, y) plane. A general particle of the cloud is at (ξ, η, ζ), and the distance from the nucleus to any particle is r_2, which is small compared with a, and with r_1, the distance to the earth of mass M located at the origin; the ratio $m/M = \beta$ is assumed to be extremely small compared with unity.

The particle (ξ, η, ζ) is attracted by m and M but does not influence their motion; m is in uniform circular motion about M. The equations of motion of a typical dust particle can be written as

$$\begin{aligned} \ddot{\xi} &= -GM\xi/r_1^3 - Gm(\xi - x)/r_2^3 \\ \ddot{\eta} &= -GM\eta/r_1^3 - Gm(\eta - y)/r_2^3 \\ \ddot{\zeta} &= -GM\zeta/r_1^3 - Gm\zeta/r_2^3 \end{aligned} \tag{1}$$

where G is the gravitational constant and $r_1^2 = \xi^2 + \eta^2 + \zeta^2$, $r_2^2 = (\xi - x)^2 + (\eta - y)^2 + \zeta^2$; $x = a\cos(kt)$, $y = a\sin(kt)$, $k^2 = GM/a^3$.

The usual uniformly rotating reference system is now introduced in which m is a fixed point on the X axis; the unit of distance is chosen to be a, and the dimensionless time $\tau = kt$ is introduced as the new independent variable, with $' = d/d\tau$;

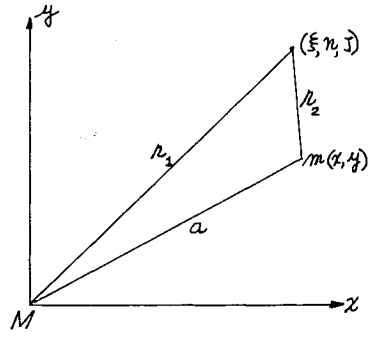

Fig. 1

Presented as Preprint 63-425 at the AIAA Astrodynamics Conference, New Haven, Conn., August 19–21, 1963; revision received July 16, 1964. The work reported upon here was begun at the Mathematics Research Center of the U. S. Army at the University of Wisconsin under Contract DA-11-022-ORD-2059 and was continued under the Air Force Office of Scientific Research Grant 598-64 at Adelphi University.

* Professor of Mathematics. Associate Fellow Member AIAA.